IEEE Access
Multidisciplinary | Rapid Review | Open Access Journal

SPECIAL SECTION ON ADVANCED BIG DATA ANALYSIS FOR VEHICULAR SOCIAL NETWORKS

Received November 19, 2018, accepted November 29, 2018, date of publication December 4, 2018, date of current version December 31, 2018.

Digital Object Identifier 10.1109/ACCESS.2018.2884957

Dynamic Stiffness Characteristics Analysis of Bogie Suspension for Rail Vehicle Based on Big Data-Driven Bench Test

ZHIHUI NIU, JIAN SU, YINRUI ZHANG, AND HUIYING LIN
College of Transportation, Jilin University, Changchun 130022, China
Corresponding author: Zhihui Niu (niuzhihui21@126.com)

This work was supported by the Natural Science Foundation of China under Grant 51575232.

ABSTRACT The vehicle test big data has important significance for the study of vehicle performance and characteristics. Aiming at the test of the dynamic stiffness characteristics of a bogie suspension system of rail vehicles, a simplified rigid-flexible hybrid model of the bogie is established, and the force condition of the bogie suspension system is analyzed. Based on this simplified model, a mathematical model of the dynamic stiffness of the primary suspension, secondary suspension, and integrated suspension is established. In addition, a method for testing the three-way dynamic stiffness of a bogie suspension system in a complete, assembled state is proposed, and a dynamic stiffness test model of the bogie primary suspension, secondary suspension, and comprehensive suspension is established. Dynamic stiffness tests of the primary suspension, secondary suspension, and integrated suspension were carried out, and according to the big data analysis of the bench test, the dynamic stiffness curve of each suspension in the frequency of 0.5–5 Hz is obtained. The test results show that the dynamic stiffness of the suspension of the bogies varies nonlinearly with the change in frequency. The dynamic stiffness values of the suspensions at different frequencies vary greatly. As a result, the vehicle's operating characteristics cannot be evaluated based on the suspension static stiffness or the suspension stiffness at a single frequency, indicating the necessity of the suspension dynamic stiffness test after the bogie is assembled.

INDEX TERMS Rail vehicle, test big data, bogie, suspension stiffness, dynamic stiffness test, stiffness characteristics.

I. INTRODUCTION

A bogie is one of the main components in ensuring the safe operation of rail vehicles. The running stability and ride comfort of the train are closely related to the suspension characteristics of the bogie [1]–[6]. The dynamic performance of a rail vehicle with a secondary suspension is directly related to primary suspension system [7], [8]. The lateral stability of the vehicle depends mainly upon the characteristics of the secondary transverse stiffness and the damping of the secondary transverse damper when the system is stabilised [9]–[13]. During the design of a bogie, the suspension stiffness parameters are derived from and optimized using theoretical calculations and software simulations. However, in the actual production of a bogie, the suspension stiffness parameters depend not only on the parameters of the corresponding suspension components but also on the assembly of the components—, and assembly error can substantially influence the suspension parameters. The suspension element stiffness and the static and dynamic characteristics of damping are also very different [14]. Therefore, the 3D dynamic stiffness of the bogie suspension system must be measured after the bogie is assembled to ensure that the suspension parameters can meet the design requirements [15]–[17].

For the determination of the suspension stiffness of the bogie, Aizpun *et al.* [18], Wang *et al.* [20], and Bideleh and Berbyuk [21] obtained the rotational stiffness parameters of a suspension system via simulation and parameter estimation. Bideleh and Berbyuk [21] and Xia *et al.* [22] analyzed the influence of suspension parameters on bogie dynamics. Li *et al.* [23], Feng *et al.* [24], Tian *et al.* [25], and Tian *et al.* [26] analyzed a type of bogie consisting of a primary suspension axle box spring. Qin Zhen et al. studied the influence of secondary suspension parameters on the critical speed of trains [27]–[29]. The bogie parameter test bench developed by Southwest Jiaotong University can test the overall stiffness of the bogie, but it is not

possible to measure the primary suspension and the secondary suspension separately [30]–[32]. HE analyzed the influence of a bending-resistant torsion bar on train dynamics [33]. Chi Maoru analyzed the influence of secondary suspension parameters on the lateral stability of the vehicle body by simulation [9], but the test method for the secondary suspension parameters of the bogie was not studied. Qi *et al.* [34], Chen *et al.* [35] conducted a dynamic study on the air springs of rail vehicles, but only performed a simulation to examine the air springs in the secondary suspension, which cannot replace testing the actual performance of the secondary suspension in its completed state. Zhang *et al.* [36] measured the one-line suspension stiffness of bogies. Shi *et al.* [37] studied the suspension stiffness characteristics of high-speed EMU bogies, and Shi *et al.* [38] tested the bogie yaw coefficient. Zhou *et al.* [39] studied the dynamic stiffness of the bearing by the spectrum analysis method. Zong *et al.* [40], Tian *et al.* [26], and Xia *et al.* [41] used the vibration transfer function analysis method to study the dynamic stiffness characteristics of the gearbox. Matsubara *et al.* [42] tested the dynamic stiffness of the spindle by applying a sine wave excitation to the machine tool spindle. LU [43] used impact technology to measure the dynamic stiffness of the engine mount. Hu *et al.* [44] studied the dynamic stiffness characteristics of the engine rubber suspension by finite element simulation and test methods. Jilin University has developed a new type of bogie test bench, which can separately determine the three-way dynamic and static stiffness suspension parameters of the secondary suspension system in a complete, assembled bogie.

This paper describes the basic structure and working principle of the test equipment of the new bogie suspension system; the main contributions of this paper can be summarized as follows:

1) Based on the structure of the bogie of the rail vehicle, the rigid-flexible model of the bogie is established, and the force condition of the bogie suspension system is analyzed.

2) According to the structure of the bogie suspension system, the mathematical model and test model of the dynamic stiffness of the suspension system are established.

3) A test method for dynamic stiffness testing of a bogie suspension system is provided;

4) The stiffness characteristics test of the bogie suspension system of the rail vehicle was carried out. The dynamic stiffness characteristics of the bogie suspension system were obtained by analyzing the dynamic test results.

II. TEST SYSTEM AND BOGIE PHYSICAL MODEL ANALYSIS

A. TEST SYSTEM

As shown in Fig 1, the physical structure of the test system serves as special equipment for track vehicle parameter detection. The bogie parameter test bench can realize the static and dynamic measurement of the suspension parameters under the condition of bogie assembly and the completion condition

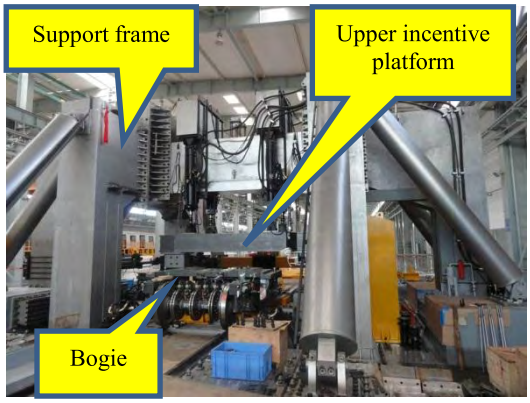

FIGURE 1. Test system physical structure.

of the whole vehicle, which can simulate the actual running condition of the vehicle, too. The test bench consists of three independent 6-DOF motion platforms and support frames. The upper 6-DOF is mounted on the support frame, and the two lower 6-DOF motion platforms are mounted on the foundation. Each of them is driven by seven servo actuators to allow the 6-DOF spatial motion. The 6-DOF excitation loading of the bogie can be performed separately, and the two lower 6-DOF motion platforms can simultaneously perform excitation loading on the bogie. The test bench has a maximum excitation force of 200 tons and a maximum excitation frequency of 15 Hz.

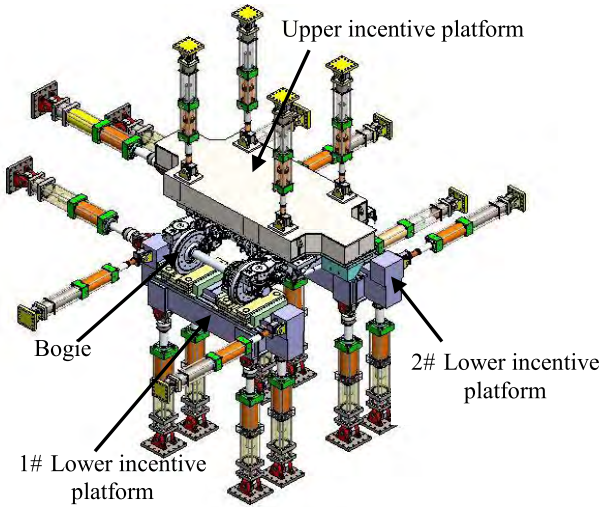

FIGURE 2. Experimental schematic of the stiffness test.

Fig 2 illustrates an experimental schematic of the stiffness test. The second wheel of the bogie is fixed to the 3D force sensor connected on the No. 1 lower excitation platform and the No. 2 lower excitation platform, and the bolster is fastened to the 3D force sensor at the lower end of the upper excitation platform. Thus, the force of the bogie wheel pair and the bolster in the three directions of X, Y and Z can be measured during the test process.

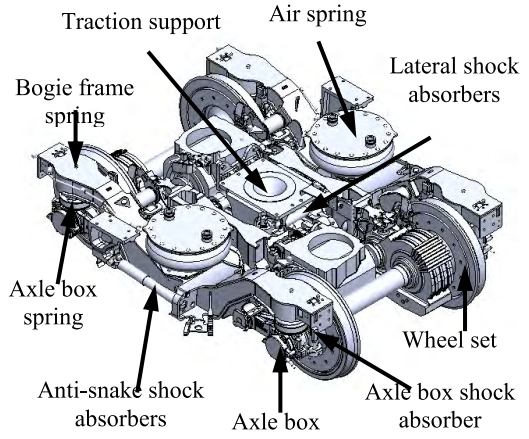

FIGURE 3. CRH3 bogie structure diagram.

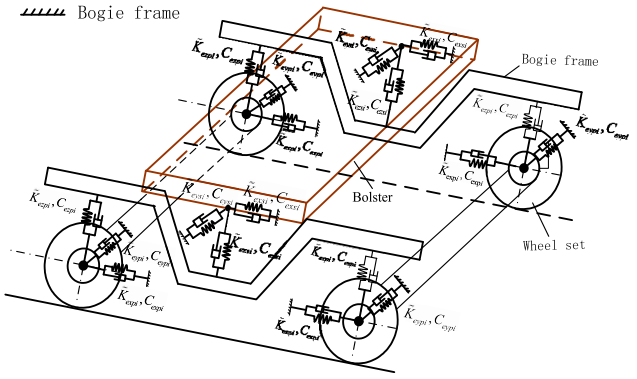

FIGURE 4. Rigid and flexible hybrid model of the bogie.

B. ANALYSIS OF THE BOGIE PHYSICAL MODEL

In this paper, the suspension stiffness characteristics of the CRH3-type bogie are studied, as shown in Fig.3. This bogie is composed of a wheelset, primary suspension, frame, secondary suspension and bolster. The primary suspension mainly consists of an axle box spring, a flexible rubber pad, a box shock absorber and an axle box positioning device. The secondary suspension of the bogie is mainly composed of air springs, lateral shock absorbers, anti-snake shock absorbers, Z-type traction rods, etc. The air spring can not only achieve elastic support in the suspension system but also provide damping. The structure of the CRH3 bogie establishes the following simplified rigid-flexible hybrid model of the bogie, as shown in Figure 4:

(1) $\tilde{K}_{expi}$, $\tilde{K}_{eypi}$, $\tilde{K}_{ezpi}$ (i=1, 2, 3, 4) are the longitudinal, lateral and vertical equivalent stiffnesses, respectively, of the four primary suspensions of the bogie.

(2) C_{expi}, C_{eypi}, C_{ezpi} (i=1, 2, 3, 4) are the longitudinal, lateral and vertical equivalent damping coefficients, respectively, of the four primary suspensions of the bogie.

(3) $\tilde{K}_{exsi}$, $\tilde{K}_{eysi}$, $\tilde{K}_{ezsi}$ (i=1, 2) are the longitudinal, lateral and vertical equivalent stiffnesses, respectively, of the two secondary suspensions of the bogie.

(4) C_{exsi}, C_{eysi}, C_{ezsi} (i=1, 2) are the longitudinal, lateral and vertical equivalent damping coefficients, respectively, of the two secondary suspensions of the bogie.

III. MATHEMATICAL MODEL AND MEASUREMENT METHOD OF THE STIFFNESS OF THE BOGIE SUSPENSION SYSTEM

A. BOGIE TEST FORCE ANALYSIS

As shown in Figure 5, simplified force analysis of the test bogie is based on the bogie structure and test plan in the test. During the test, the bogie is under the gravity of $m_{w1}g$ and $m_{w2}g$ of the two wheelset; the frame gravity m_Bg; the loading force of upper excitation platform exerted to the secondary suspension F_{Xsi} $(i = 1, 2)$, F_{Ysi} $(i = 1, 2)$, F_{Zsi} $(i = 1, 2)$; the loading force of the wheelset of lower excitation platform exerted to the primary suspension F_{Xpi} $(j = 1, 2, 3, 4)$, F_{Ypi} $(j = 1, 2, 3, 4)$, F_{Zpi} $(j = 1, 2, 3, 4)$; the supporting force of the frame supporting device to the frame F_{XBk} $(k = 1, 2, 3, 4)$, F_{YBk} $(k = 1, 2, 3, 4)$, F_{ZBk} $(k = 1, 2, 3, 4)$, thus the balance equation of each force of the bogie is obtained according to the force balance:

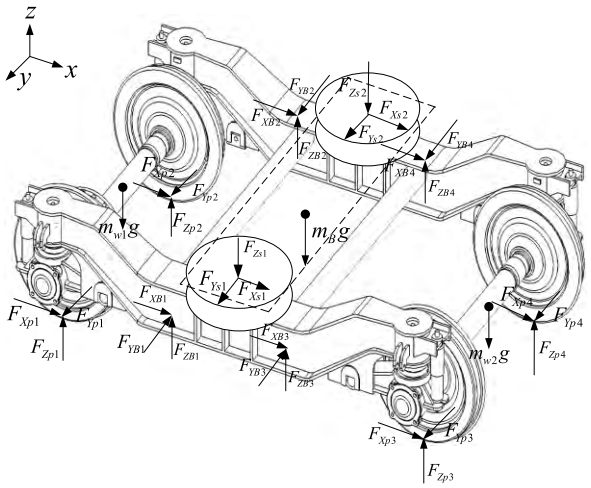

FIGURE 5. Force diagram of bogie simplified model.

Longitudinal:

$$\sum_{i=1}^{2} F_{Ysi} + \sum_{j=1}^{4} F_{Ypj} + \sum_{k=1}^{4} F_{YBk} = 0 \tag{1}$$

Lateral:

$$\sum_{i=1}^{2} F_{Xsi} + \sum_{j=1}^{4} F_{Xpj} + \sum_{k=1}^{4} F_{XBk} = 0 \tag{2}$$

Vertical:

$$\sum_{i=1}^{2} F_{ZSi} + \sum_{j=1}^{4} F_{Zpj} + \sum_{k=1}^{4} F_{ZBk} + m_{w1}g + m_{w2}g + m_Bg = 0 \tag{3}$$

B. MATHEMATICAL MODEL OF THE DYNAMIC STIFFNESS OF THE SUSPENSION

1) MATHEMATICAL MODEL FOR TESTING THE DYNAMIC STIFFNESS OF THE PRIMARY SUSPENSION AND SECONDARY SUSPENSION

The structure and composition of the primary suspension and the secondary suspension reveal that both suspensions are spring-damped systems. The mathematical model of the lateral, longitudinal and vertical dynamic stiffness of the bogie primary suspension and the lateral, longitudinal and vertical dynamic stiffness of the bogie secondary suspension can be expressed as a single-degree-of-freedom spring-mass system, as shown in Fig 6.

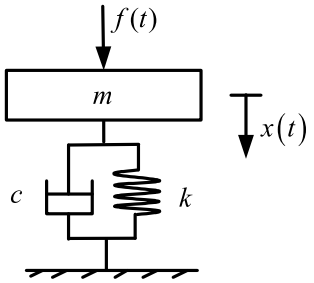

FIGURE 6. Mathematical model of the dynamic stiffness test for the first and second suspensions of the bogie.

In the dynamic stiffness test, a simple harmonic excitation is applied to the bogie system. According to Newton's second law, the differential equation of motion of the single-degree-of-freedom spring damping system is:

$$m\ddot{x}(t) + c\dot{x}(t) + kx(t) = f(t) \tag{4}$$

If the excitation is given by $f(t) = Fe^{jwt}$ and the response by $x(t) = Xe^{jwt}$, then the system's displacement frequency response function will be:

$$H(\omega) = \frac{X}{F} = \frac{1}{k - m\omega^2 + jc\omega} \tag{5}$$

The dynamic stiffness is the ratio of force to displacement:

$$K_d(\omega) = \frac{F}{X} = k - m\omega^2 + jc\omega \tag{6}$$

This formula shows that the dynamic stiffness $K_d(\omega)$ is a function of frequency ω and not a fixed value. The stiffness at a particular frequency depends on the static stiffness k, damping c and mass m of the system.

The dynamic stiffness of primary suspensions is:

$$K_{pdi}(\omega) = k_{pi} - m_{pi}\omega^2 + jc_{pi}\omega, \quad (i = 1, 2, 3, 4) \tag{7}$$

The dynamic stiffness of secondary suspensions is:

$$K_{Sdi}(\omega) = k_{Si} - m_{Si}\omega^2 + jc_{Si}\omega, \quad (i = 1, 2) \tag{8}$$

2) MATHEMATICAL MODEL OF THE COMPREHENSIVE DYNAMIC STIFFNESS OF THE BOGIE

According to the physical model analysis of the bogie, the lateral, longitudinal and vertical integrated suspension systems of the bogie are all two-degrees-of-freedom spring-mass systems with viscous damping. The lateral, longitudinal and vertical integrated suspension systems of the bogie can be expressed as the two-degrees-of-freedom spring mass system shown in Fig 7.

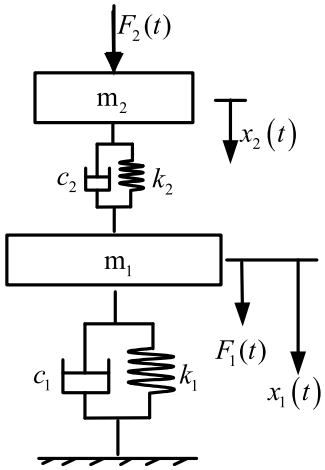

FIGURE 7. Mathematical model of the comprehensive dynamic stiffness test for the bogie suspension.

Harmonic excitation is applied to the bogie system during the dynamic stiffness test. According to Newton's second law, the differential equation of motion of the two-degrees-of-freedom spring-mass system is:

$$\begin{cases} m_1\ddot{x}_1 + (c_1 + c_2)\dot{x}_1 - c_2\dot{x}_2 + (k_1 + k_2)x_1 - k_2x_2 = F_1(t) \\ m_2\ddot{x}_2 - c_2\dot{x}_1 + c_2\dot{x}_2 - k_2x_1 + k_2x_2 = F_2(t) \end{cases} \tag{9}$$

where $c_1 = c_{ep1} + c_{ep2} + c_{ep3} + c_{ep4}$ and $c_2 = c_{es1} + c_{es2}$.

The two simultaneous second-order ordinary differential equations above can be expressed in matrix form [45] as follows:

$$[m]\{\ddot{x}(t)\} + [c]\{\dot{x}(t)\} + [k]\{x(t)\} = \{F(t)\} \tag{10}$$

In the above formula,

$$[m] = \begin{bmatrix} m_1 & 0 \\ 0 & m_2 \end{bmatrix},$$

$$[c] = \begin{bmatrix} c_1 + c_2 & -c_2 \\ -c_2 & c_2 \end{bmatrix},$$

$$[k] = \begin{bmatrix} k_1 + k_2 & -k_2 \\ -k_2 & k_2 \end{bmatrix},$$

$$\{x(t)\} = \begin{Bmatrix} x_1(t) \\ x_2(t) \end{Bmatrix},$$

$$\{F(t)\} = \begin{Bmatrix} F_1(t) \\ F_2(t) \end{Bmatrix}$$

Equation (9) is rewritten as follows:

$$\begin{cases} m_{11}\ddot{x}_1 + m_{12}\ddot{x}_2 + c_{11}\dot{x}_1 + c_{12}\dot{x}_2 + k_{11}x_1 + k_{12}x_2 = F_1(t) \\ m_{12}\ddot{x}_1 + m_{22}\ddot{x}_2 + c_{12}\dot{x}_1 + c_{22}\dot{x}_2 + k_{12}x_1 + k_{12}x_2 = F_2(t) \end{cases} \tag{11}$$

The harmonic excitation is rewritten as follows:

$$F_1(t) = F_1 e^{jwt}, \quad F_2(t) = F_2 e^{jwt} \tag{12}$$

Then, the corresponding response is:

$$x_1(t) = X_1 e^{jwt}, \quad x_2(t) = X_2 e^{jwt} \tag{13}$$

Combining equations (12) and (13) with equation (11):

$$\begin{cases} \left(-\omega^2 m_{11} + j\omega c_{11} + k_{11}\right) X_1 \\ \quad + \left(-\omega^2 m_{12} + j\omega c_{12} + k_{12}\right) X_2 = F_1 \\ \left(-\omega^2 m_{12} + j\omega c_{12} + k_{12}\right) X_1 \\ \quad + \left(-\omega^2 m_{22} + j\omega c_{22} + k_{22}\right) X_2 = F_2 \end{cases} \tag{14}$$

Assuming, $Z_{ik}(\omega) = -\omega^2 m_{ik} + j\omega c_{ik} + k_{ik}$ $(i, k = 1, 2)$.

Equation (14) can be converted into matrix form:

$$[Z(\omega)]\{X\} = \{F\} \tag{15}$$

From this, the following can be obtained:

$$\{X\} = [Z(\omega)]^{-1}\{F\} \tag{16}$$

Among these:

$$\begin{aligned} &[Z(\omega)]^{-1} \\ &= \frac{1}{\det[Z(\omega)]} \begin{bmatrix} Z_{22}(\omega) & -Z_{12}(\omega) \\ -Z_{12}(\omega) & Z_{11}(\omega) \end{bmatrix} \\ &= \frac{1}{Z_{11}(\omega) Z_{22}(\omega) - Z_{12}^2(\omega)} \begin{bmatrix} Z_{22}(\omega) & -Z_{12}(\omega) \\ -Z_{12}(\omega) & Z_{11}(\omega) \end{bmatrix} \end{aligned}$$

Therefore,

$$X_1 = \frac{Z_{22}(\omega) F_1 - Z_{12}(\omega) F_2}{Z_{11}(\omega) Z_{22}(\omega) - Z_{12}^2(\omega)} \tag{17}$$

$$X_2 = \frac{-Z_{12}(\omega) F_1 + Z_{11}(\omega) F_2}{Z_{11}(\omega) Z_{22}(\omega) - Z_{12}^2(\omega)} \tag{18}$$

In the comprehensive dynamic stiffness test of the bogie, as shown in Fig 7, $F_1(t) = 0$. Thus, the integrated dynamic stiffness of the bogie may be obtained from equation (18):

$$\begin{aligned} &K_{ed}(\omega) \\ &= \frac{F_2}{X_2} = \frac{Z_{11}(\omega) Z_{22}(\omega) - Z_{12}^2(\omega)}{Z_{11}(\omega)} \\ &= \frac{\left(-\omega^2 m_{11} + j\omega c_{11} + k_{11}\right)\left(-\omega^2 m_{22} + j\omega c_{22} + k_{22}\right)}{-\omega^2 m_{11} + j\omega c_{11} + k_{11}} \\ &\quad - \frac{\left(-\omega^2 m_{12} + j\omega c_{12} + k_{12}\right)^2}{-\omega^2 m_{11} + j\omega c_{11} + k_{11}} \end{aligned} \tag{19}$$

C. SUSPENSION DYNAMIC STIFFNESS EXPERIMENTAL TEST AND METHOD

When the dynamic stiffness of the bogie suspension system is tested, a steady-state sinusoidal excitation is applied to the suspension system, after which the measured force and displacement at a given excitation frequency are calculated to obtain the dynamic stiffness at that frequency. The stiffness characteristics of the suspension systems at different frequencies are determined by applying different excitation frequencies to the suspension system [46], [47].

1) VERTICAL COMPREHENSIVE DYNAMIC STIFFNESS TEST MODEL AND TEST METHOD

The test of the vertical comprehensive dynamic stiffness of the bogie suspension is carried out with the bogie frame unconstrained, and a vertical sinusoidal excitation is applied to the bolster or to the secondary suspension through the test rig. Fig 8 shows the dynamic test model for comprehensive vertical stiffness. In the figure, $\tilde{F}_{Zs1}$ and $\tilde{F}_{Zs2}$ are the vertical dynamic excitations acting on the bogie suspension system, where $\tilde{F}_{Zsi} = F_{Zsi} I(t)$, and $I(t)$ is the periodic excitation function. Based on the analysis of the bogie test force model and considering the influence of nonlinear factors, the following is obtained:

$$F_{Zc} = K_{Zc} S_{Zc} + C_{Zc} \dot{S}_{Zc} + \Theta F_{Zc} \tag{20}$$

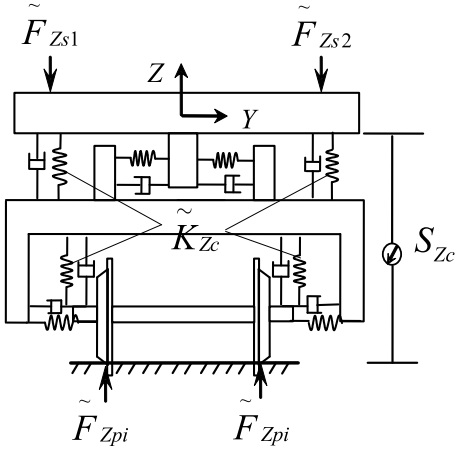

FIGURE 8. Comprehensive Vertical dynamic stiffness test model for the bogie suspension.

In the above formula:

$$F_{Zc} = F_{Zp1} + F_{Zp2} + F_{Zp3} + F_{Zp4}$$

(1) ΘF_{Zc} is the nonlinear force of the overall suspension in the vertical direction.

(2) C_{Zc} is the overall suspension damping coefficient.

(3) $\tilde{F}_{Zpi}$ is the load on the four wheels measured during the test.

After the vertical dynamic load for each suspension is stabilised, the internal force of the suspension is equal to the measured value under the steady-state excitation load,

assuming that $\delta_{Zc} = [S_{Zc}(\infty) - S_{Zc}(0)]$, and the vertical integrated dynamic stiffness $\tilde{K}_{Zc}$ of the suspension can be expressed as:

$$\tilde{K}_{Zc} = \frac{\tilde{F}_{Zc}}{\delta_{Zc}} = \frac{F_{Zc}I(\infty) - F_{Zc}I(0)}{S_{Zc}(\infty) - S_{Zc}(0)} \tag{21}$$

In this formula:

(1) $F_{Zc}I(\infty)$ is the comprehensive steady-state load maximum value of the wheel measured in the vertical direction.

(2) $F_{Zc}I(0)$ is the comprehensive steady-state load minimum value of the wheel measured in the vertical direction.

(3) $S_{Zc}(\infty)$ is the vertical integrated deflection corresponding to the maximum value of the steady state load.

(4) $S_{Zc}(0)$ is the vertical integrated deflection corresponding to the minimum value of the steady state load.

In the same way, the lateral dynamic excitation load and the longitudinal dynamic excitation load are applied to the bogie using the method for comprehensive vertical dynamic stiffness measurement, and the comprehensive lateral dynamic stiffness of the bogie suspension $\tilde{K}_{Yc}$ and the comprehensive longitudinal dynamic stiffness of the suspension $\tilde{K}_{Xc}$ can be obtained.

$$\tilde{K}_{Yc} = \frac{\tilde{F}_{Yc}}{\delta_{Yc}} = \frac{F_{Yc}I(\infty) - F_{Yc}I(0)}{S_{Yc}(\infty) - S_{Yc}(0)} \tag{22}$$

In this formula:

(1) $F_{Yc}I(\infty)$ is the comprehensive steady-state load maximum value of the wheel measured in the lateral direction.

(2) $F_{Yc}I(0)$ is the comprehensive steady-state load minimum value of the wheel measured in the lateral direction.

(3) $S_{Yc}(\infty)$ is the lateral integrated deflection corresponding to the maximum value of the steady state load.

(4) $S_{Yc}(0)$ is the lateral integrated deflection corresponding to the minimum value of the steady state load.

$$\tilde{K}_{Xc} = \frac{\tilde{F}_{Xc}}{\delta_{Xc}} = \frac{F_{Xc}I(\infty) - F_{Xc}I(0)}{S_{Xc}(\infty) - S(0)_{Xc}} \tag{23}$$

In this formula:

(1) $F_{Xc}I(\infty)$ is the comprehensive steady-state load maximum value of the wheel measured in the longitudinal direction.

(2) $F_{Xc}I(0)$ is the comprehensive steady-state load minimum value of the wheel measured in the longitudinal direction.

(3) $S_{Xc}(\infty)$ is the longitudinal integrated deflection corresponding to the maximum value of the steady state load.

(4) $S_{Xc}(0)$ is the longitudinal integrated deflection corresponding to the minimum value of the steady state load.

2) TEST MODEL AND METHOD FOR VERTICAL DYNAMIC STIFFNESS TEST OF THE PRIMARY SUSPENSION

For the $\tilde{K}_{Zpi}$ test, the tool is used to fix the two sides of the frame to the foundation, and a vertical sinusoidal excitation is applied to the primary suspension through the test bench.

Fig 9 shows the dynamic test model of the vertical stiffness of the primary suspensions. In the figure, $\tilde{F}_{Zpi}$ is the vertical

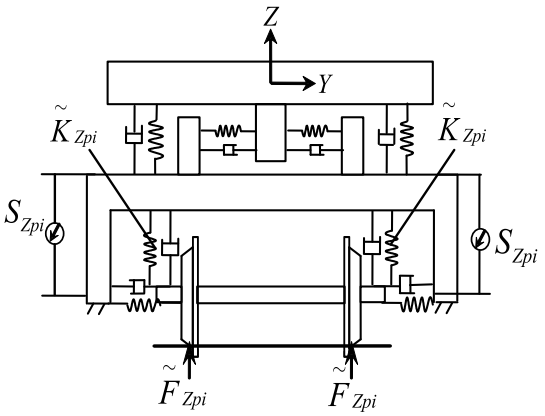

FIGURE 9. Vertical dynamic stiffness test model for the bogie primary suspension.

dynamic excitation load acting on the primary suspension of a series, and $\tilde{F}_{Zpi} = F_{Zpi}I(t)$ and $I(t)$ are the periodic excitation functions. According to the analysis of the internal force model of the bogie and considering the effects of nonlinear factors, the following is obtained:

$$F_{Zpi} = K_{Zpi} \cdot S_{Zpi} + C_{Zpi} \cdot \dot{S}_{Zpi} + \Theta F_{Zpi} \quad (i = 1, 2, 3, 4) \tag{24}$$

In the formula, ΘF_{Zpi} are the four forces that are suspended in the vertical direction of the nonlinear force.

As the vertical dynamic load for each primary suspension reaches the steady state, the internal force of each suspension becomes equal to the dynamic load acting on it. If $\delta_{Zpi} = [S_{Zpi}(\infty) - S_{Zpi}(0)]$, the vertical dynamic stiffness $\tilde{K}_{Zpi}$ of each primary suspension can be expressed as:

$$\tilde{K}_{Zpi} = \frac{\tilde{F}_{Zpi}}{\delta_{Zpi}} = \frac{F_{Zpi}I(\infty) - F_{Zpi}I(0)}{S_{Zpi}(\infty) - S_{Zpi}(0)} \tag{25}$$

In the above formula (19):

(1) $F_{Zpi}I(\infty)$ is the measured maximum steady-state load of the primary suspension in the vertical direction.

(2) $F_{Zpi}I(0)$ is the measured minimum steady-state load of the primary suspension in the vertical direction.

(3) $S_{Zpi}(\infty)$ is the corresponding vertical deflection of the primary suspension when the steady state load reaches its maximum value.

(4) $S_{Zpi}(0)$ is the corresponding vertical deflection of the primary suspension when the steady state load reaches its minimum value.

In the same way, The lateral dynamic excitation load and the longitudinal dynamic excitation load are applied to the suspension of primary suspensions by a method used for vertical dynamic stiffness measurement. The lateral dynamic stiffness $\tilde{K}_{Ypi}$ and longitudinal dynamic stiffness $\tilde{K}_{Xpi}$ of the primary suspension of the bogie are thus obtained.

$$\tilde{K}_{Ypi} = \frac{\tilde{F}_{Ypi}}{\delta_{Ypi}} = \frac{F_{Ypi}I(\infty) - F_{Ypi}I(0)}{S_{Ypi}(\infty) - S_{Ypi}(0)} \tag{26}$$

In this formula:

(1) $F_{Ypi}I(\infty)$ is the measured maximum steady-state load of the primary suspension in the lateral direction.

(2) $F_{Ypi}I(0)$ is the measured minimum steady-state load of the primary suspension in the lateral direction.

(3) $S_{Ypi}(\infty)$ is the corresponding lateral deflection of the primary suspension when the steady state load reaches its maximum value.

(4) $S_{Ypi}(0)$ is the corresponding lateral deflection of the primary suspension when the steady state load reaches its minimum value.

$$\tilde{K}_{Xpi} = \frac{\tilde{F}_{Xpi}}{\delta_{Ypi}} = \frac{F_{Xpi}I(\infty) - F_{Xpi}I(0)}{S_{Xpi}(\infty) - S_{Xpi}(0)} \tag{27}$$

In this formula:

(1) $F_{Ypi}I(\infty)$ is the measured maximum steady-state load of the primary suspension in the longitudinal direction.

(2) $F_{Ypi}I(0)$ is the measured minimum steady-state load of the primary suspension in the longitudinal direction.

(3) $S_{Ypi}(\infty)$ is the corresponding longitudinal deflection of the primary suspension when the steady state load reaches its maximum value.

(4) $S_{Ypi}(0)$ is the corresponding longitudinal deflection of the primary suspension when the steady state load reaches its minimum value.

3) SECONDARY SUSPENSION VERTICAL DYNAMIC STIFFNESS TEST MODEL AND TEST METHOD

Fig 10 shows the test model for the vertical dynamic stiffness of the secondary suspension of the bogie. The bogie is fixed to the foundation of the test bench, and the vertical dynamic excitation load of the test platform is applied to the secondary suspension of the bogie. The vertical deflection of the secondary suspension of the bogie and the vertical reaction of the secondary suspension are tested in real time. In Fig 10, $\tilde{F}_{Zsi}$ is the vertical dynamic excitation load acting on the secondary suspension, where $\tilde{F}_{Zsi} = F_{Zsi}I(t)$ and $I(t)$ is the periodic excitation function. According to the analysis of the internal force model of the bogie, and considering the effects of nonlinear factors:

$$F_{Zi} = K_{Zsi} \cdot S_{Zsi} + C_{Zsi} \cdot S_{Zsi} + \Theta F_{Zsi} \quad (i = 1, 2) \tag{28}$$

In this formula:

(1) C_{Zsi} is the secondary suspension damping coefficient

(2) ΘF_{Zsi} are the nonlinear reaction forces of the secondary suspension in the vertical direction.

After the vertical dynamic load on the secondary suspension reaches the steady state, the internal force of each suspension becomes equal to the dynamic load acting on it. If $\delta_{Zsi} = [S_{Zsi}(\infty) - S_{Zsi}(0)]$, the vertical dynamic stiffness of the secondary suspension can be expressed as follows:

$$\tilde{K}_{Zsi} = \frac{\tilde{F}_{Zsi}}{\delta_{Zsi}} = \frac{F_{Zsi}I(\infty) - F_{Zsi}I(0)}{S_{Zsi}(\infty) - S_{Zsi}(0)} \tag{29}$$

In this formula:

(1) $F_{Zsi}I(0)$ is the measured minimum steady-state load of the secondary suspension in the vertical direction.

(2) $F_{Zsi}I(\infty)$ is the measured maximum steady-state load of the secondary suspension in the vertical direction.

(3) $S_{Zsi}(0)$ is the corresponding vertical deflection of the secondary suspension when the steady state load reaches its minimum value.

(4) $S_{Zsi}(\infty)$ is the corresponding vertical deflection of the secondary suspension when the steady state load reaches its maximum value.

In the same way, the lateral dynamic excitation load and the longitudinal dynamic excitation load are applied to the secondary suspension separately by the method of secondary suspension vertical dynamic stiffness measurement. From this, the lateral dynamic stiffness $\tilde{K}_{Ysi}$ and longitudinal dynamic stiffness $\tilde{K}_{Xsi}$ of the bogie secondary suspension can be obtained.

$$\tilde{K}_{Ysi} = \frac{\tilde{F}_{Ysi}}{\delta_{Ysi}} = \frac{F_{Ysi}I(\infty) - F_{Ysi}I(0)}{S_{Ysi}(\infty) - S_{Ysi}(0)} \tag{30}$$

In this formula:

(1) $F_{Ysi}I(0)$ is the measured minimum steady-state load of the secondary suspension in the lateral direction.

(2) $F_{Ysi}I(\infty)$ is the measured maximum steady-state load of the secondary suspension in the lateral direction

(3) $S_{Ysi}(0)$ is the corresponding lateral deflection of the secondary suspension when the steady state load reaches its minimum value.

(4) $S_{Ysi}(\infty)$ is the corresponding lateral deflection of the secondary suspension when the steady state load reaches its maximum value.

$$\tilde{K}_{Xsi} = \frac{\tilde{F}_{Xsi}}{\delta_{Xsi}} = \frac{F_{Xsi}I(\infty) - F_{Xsi}I(0)}{S_{Xsi}(\infty) - S_{Xsi}(0)} \tag{31}$$

In this formula:

(1) $F_{Xsi}I(0)$ is the measured minimum steady-state load of the secondary suspension in the longitudinal direction.

(2) $F_{Xsi}I(\infty)$ is the measured maximum steady-state load of the secondary suspension in the longitudinal direction

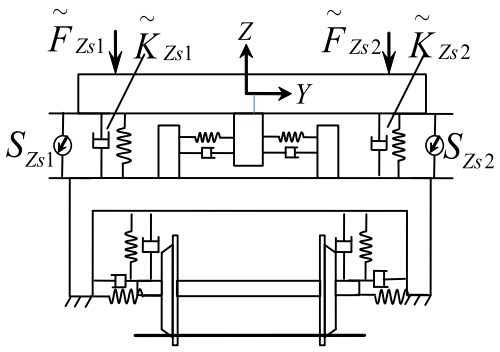

FIGURE 10. Vertical dynamic stiffness test model for bogie secondary suspension.

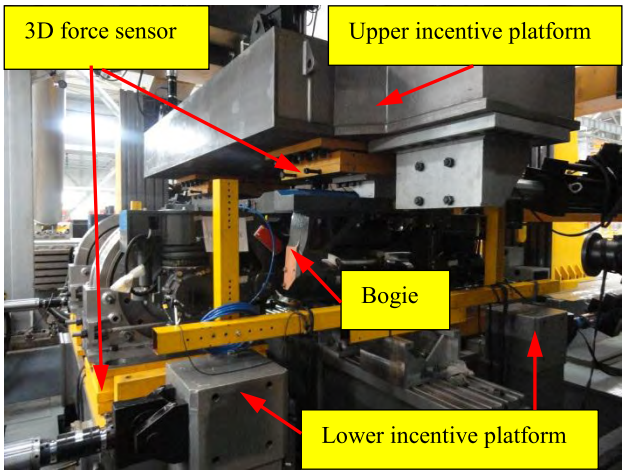

FIGURE 11. Physical structure of bogie suspension dynamic stiffness test.

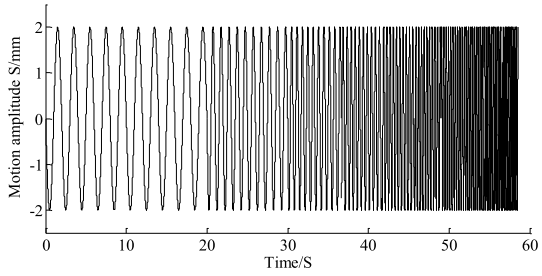

FIGURE 12. Excitation motion waveform when measuring the dynamic stiffness of the suspension.

(3) $S_{Xsi}(0)$ is the corresponding longitudinal deflection of the secondary suspension when the steady state load reaches its minimum value.

(4) $S_{Xsi}(\infty)$ is the corresponding longitudinal deflection of the secondary suspension when the steady state load reaches its maximum value.

IV. DETERMINATION OF THE DYNAMIC STIFFNESS OF THE BOGIE SUSPENSION

As shown in Figure 11, the four wheels are placed on the four force sensors separately during the bogie test, and the force sensor is connected to the lower excitation platform. The upper end of the secondary suspension connected to the upper excitation platform with two force sensors.

The laser displacement sensor is connected to the test bench base through the sensor support frame, which ensures that the laser displacement sensor is not affected by the movement of the test platform during the test. The detection accuracy of the force sensor is $\pm 2\mu$m, and the detection accuracy of the force sensor is $\pm$1kg.In the dynamic stiffness measurement test of the bogie suspension, the motion platform drives the bogie suspension system with a sine wave possessing a 2 mm amplitude, and the sweep frequency excitation test is performed with a vibration frequency interval of 0.5 Hz for a range of frequencies from 0.5 Hz to 5 Hz. The force sensor and the displacement sensor are used to measure the force

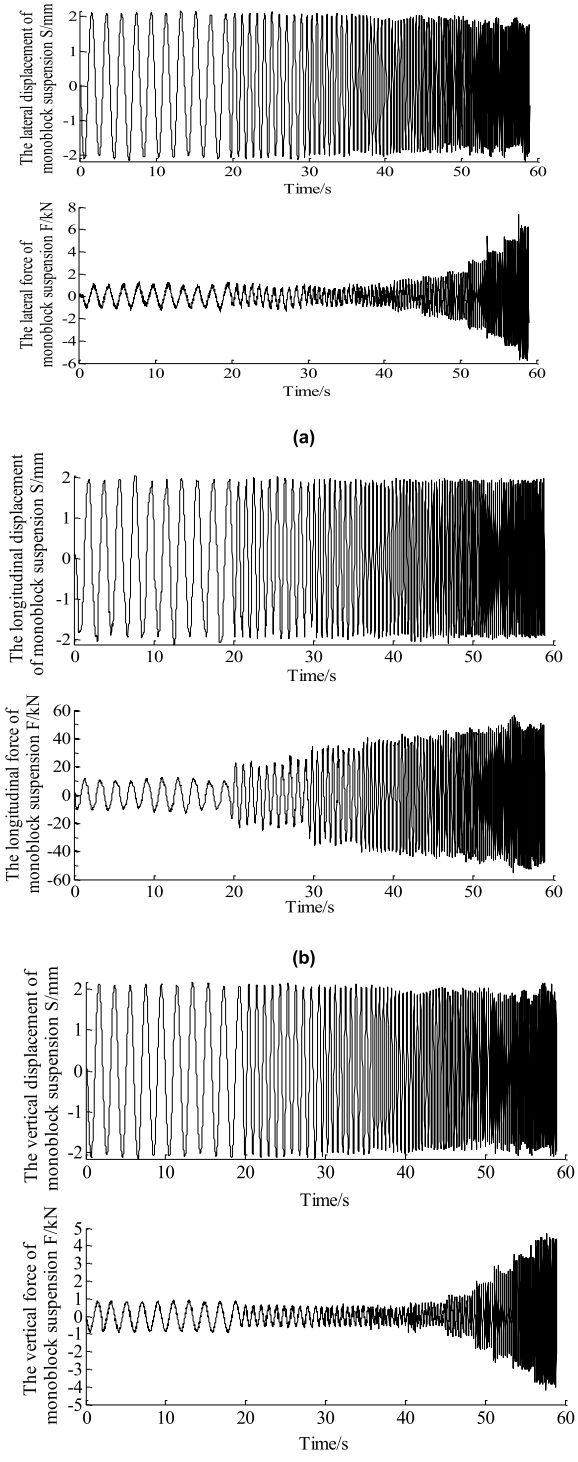

FIGURE 13. Suspension lateral comprehensive dynamic stiffness test duration curve. (a) Lateral dynamic stiffness test duration curve. (b) Longitudinal dynamic stiffness test duration curve. (c) Vertical dynamic stiffness test duration curve.

of the suspension system and the corresponding deflection, respectively, during the movement, and the dynamic stiffness is calculated from the test measurement data. The excitation motion waveform during dynamic stiffness measurement is shown in Fig12.

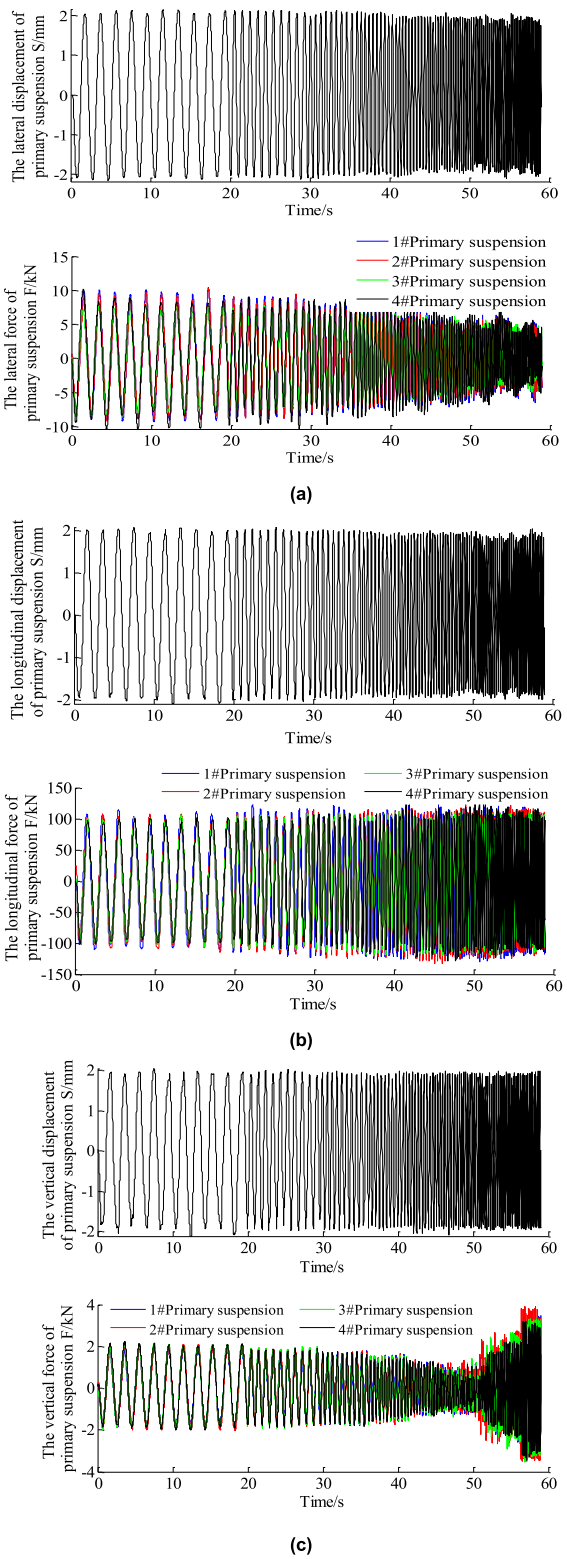

FIGURE 14. Primary suspension lateral dynamic stiffness test duration curve. (a) Lateral dynamic stiffness test duration curve. (b) Longitudinal dynamic stiffness test duration curve. (c) Vertical dynamic stiffness test duration curve.

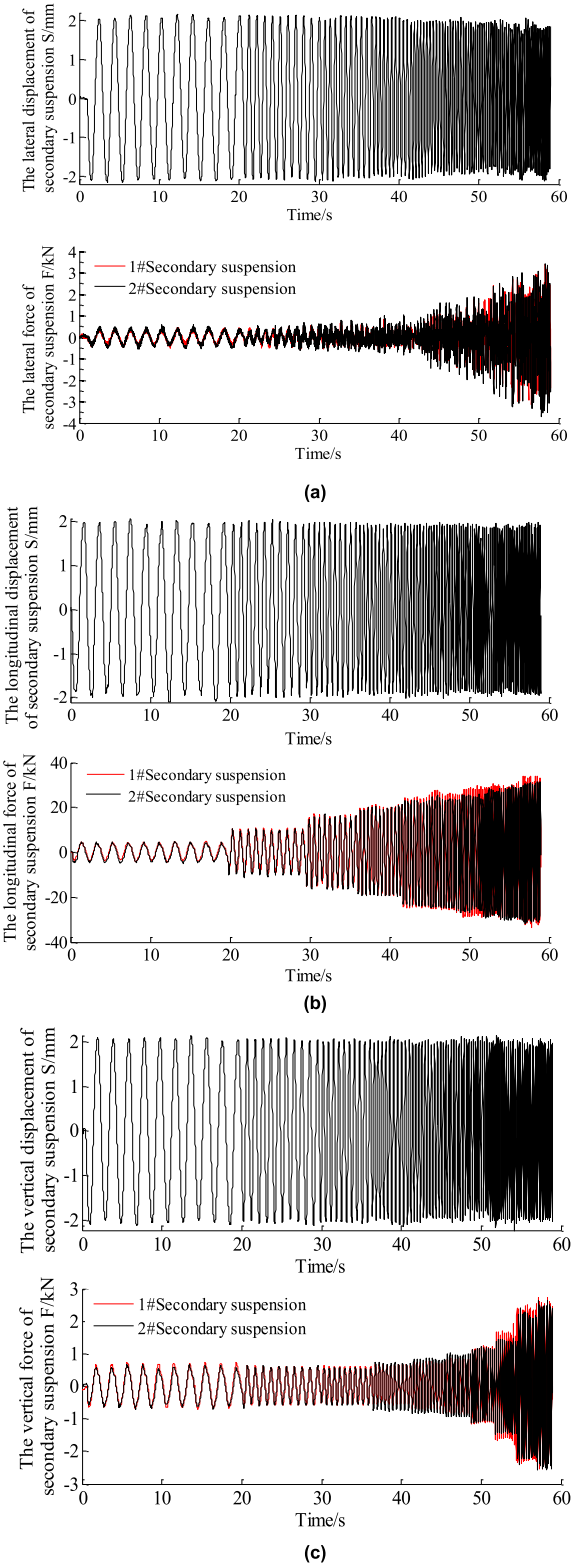

FIGURE 15. Secondary suspension lateral dynamic stiffness test duration curve. (a) Lateral dynamic stiffness test duration curve. (b) Longitudinal dynamic stiffness test duration curve. (c) Vertical dynamic stiffness test duration curve.

Fig. 13, Fig. 14 and Fig. 15 can present the measured values of the force and deformation at different frequencies of the whole suspension, primary suspension and the secondary suspension in the transverse, longitudinal and vertical directions respectively. When the motion platform travels in a sine wave, the measured values of the three-dimensional

force measuring device and the laser displacement sensor are synchronously changed, thus the stiffness values at different frequencies in the transverse, longitudinal and vertical directions of the whole suspension, the primary suspension and the secondary suspension of the bogie are obtained, and finally the dynamic stiffness characteristics of the bogie suspension system are acquired.

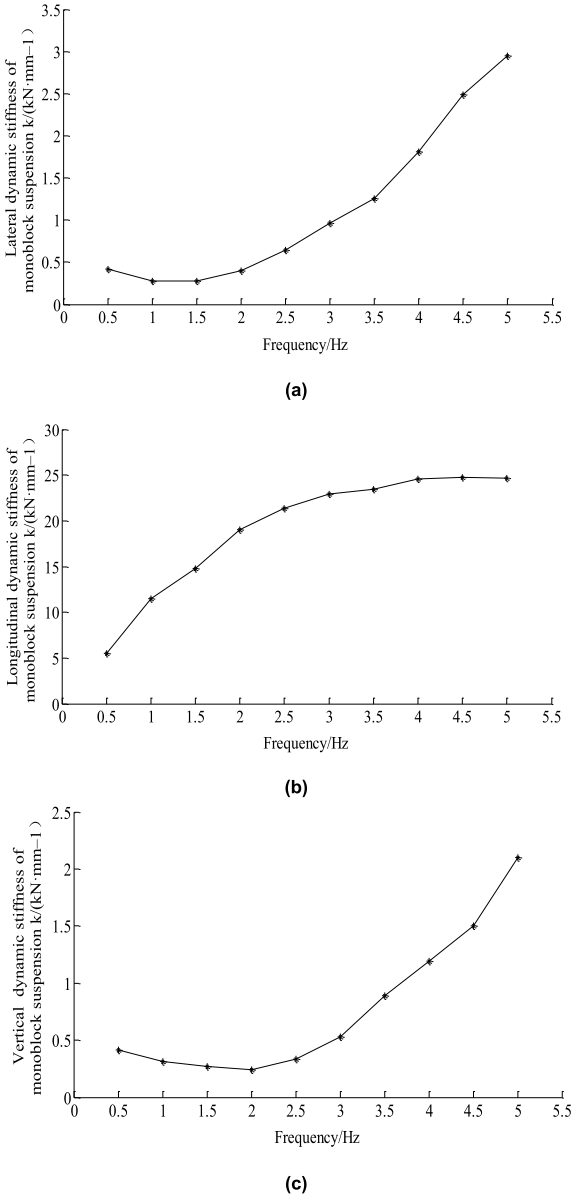

FIGURE 16. Suspension comprehensive dynamic stiffness test curves. (a) Lateral dynamic stiffness test curve. (b) Longitudinal dynamic stiffness test curve. (c) Vertical dynamic stiffness test curve.

As seen in Fig 16(a), the lateral dynamic stiffness of the suspension is in the frequency range of 0.5∼5 Hz, which first decreases with increasing frequency, where the inflection point appears at approximately 1.5 Hz, and then gradually increases with increasing frequency, where the rate of change in stiffness gradually increases with increasing frequency.

As seen in Fig 16(b), the longitudinal integrated dynamic stiffness value of the suspension is in the frequency range of 0.5∼5 Hz, and gradually increases with increasing frequency. At approximately 4 Hz, the stiffness tends to stabilize as the frequency continues to change.

As seen in Fig 16(c), the vertical dynamic stiffness of the suspension is in the frequency range of 0.5∼5 Hz. It first decreases with increasing frequency, then gradually increases with increasing frequency; the inflection point appears at approximately 2 Hz. The rate of change in stiffness gradually increases with increasing frequency.

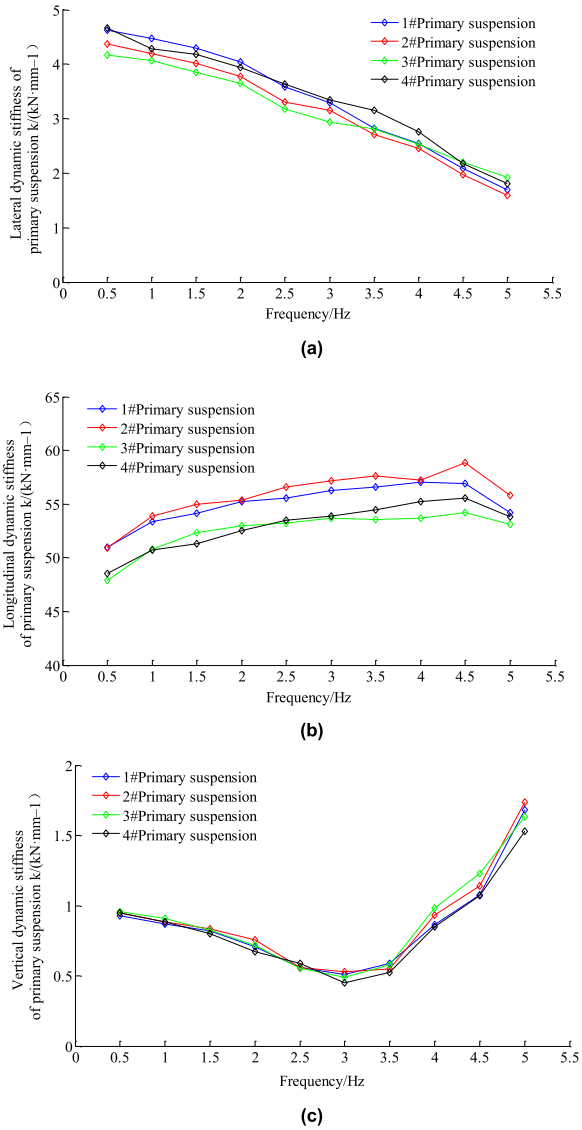

FIGURE 17. Secondary suspension lateral dynamic stiffness test duration curve. (a) Lateral dynamic stiffness test curve. (b) Longitudinal dynamic stiffness test curve. (c) Vertical dynamic stiffness test curve.

As seen in Fig 17(a), the lateral dynamic stiffness of the four primary suspensions decreases with increasing frequency in the range of 0.5∼5 Hz. The dynamic stiffness curves of the four primary suspensions are essentially identical; the transverse dynamic stiffness values of #1 and

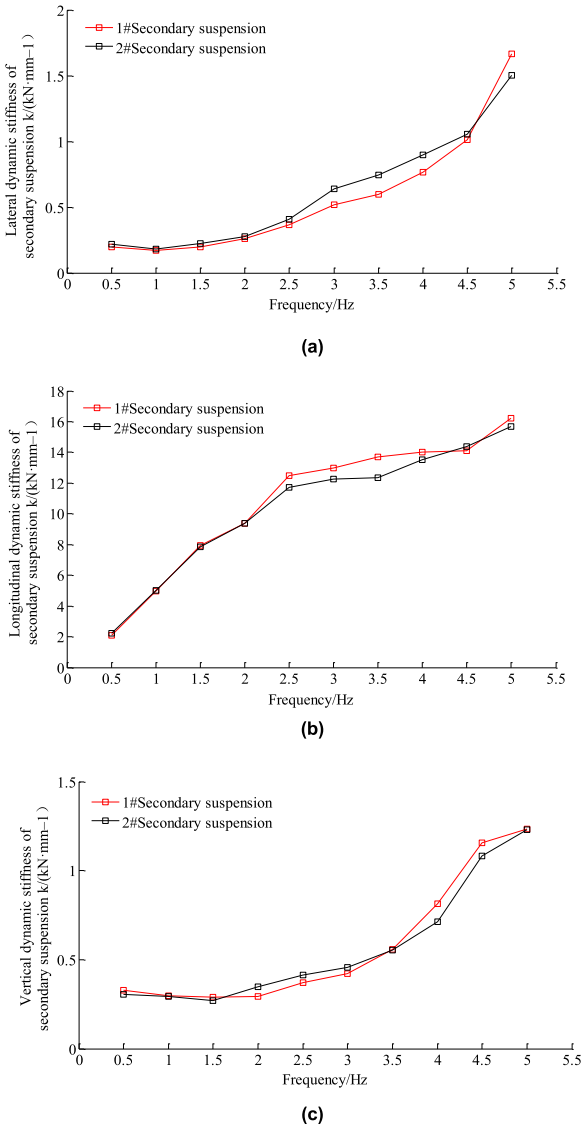

FIGURE 18. Secondary suspension vertical dynamic stiffness test curve. (a) Lateral dynamic stiffness test curve. (b) Longitudinal dynamic stiffness test curve. (c) Vertical dynamic stiffness test curve.

#4primary suspensions at the same disturbance frequency are higher than those of the 2# and 3# suspensions.

As seen in Fig 17(b), the longitudinal dynamic stiffness of the four primary suspensions is in the frequency range of 0.5∼5 Hz, which initially increases gradually with increasing frequency, , and the inflection point appears at approximately 4.5 Hz, then gradually decreases with increasing frequency. The longitudinal dynamic stiffness values of the #1 and #2 primary suspensions are greater than the longitudinal dynamic stiffness values of the #3 and #4 primary suspensions at the same disturbance frequency. Moreover, there is an unbalanced vertical dynamic stiffness parameter matching of the #1, #2 #3, and #4 suspensions. It is presumed that the test result is due to the assembly gap and the uneven distribution of the wheel mass.

As seen in Fig 17(c), the vertical dynamic stiffness of the four singe stage suspensions initially decreases with the increase in frequency in the frequency range of 0.5∼5 Hz, then gradually increases with the increase of frequency the inflection point appears at approximately 3 Hz. The dynamic stiffness curves of the four suspensions are consistent with one another.

As seen in Fig 18(a), the lateral dynamic stiffness of the #1 and #2 secondary suspensions increases with frequency in the range of 0.5∼5 Hz, and the dynamic stiffness curves of the two secondary suspensions are essentially identical.

As seen in Fig 18(b), the longitudinal dynamic stiffness of the #1 and #2 secondary suspensions increases gradually with frequency in the frequency range of 0.5∼5 Hz, and the dynamic stiffness curves of the two secondary suspensions change uniformly. The rate of change of the stiffness frequency tends to remain steady after 2.5 Hz.

As seen in Fig 18(c), the vertical dynamic stiffness of the #1 and #2 secondary suspensions is essentially stable in the frequency range of 0.5∼2 Hz, and the dynamic stiffness values of the two secondary suspensions increase with an increase in frequency in the range of 2∼5 Hz. The rate of growth gradually increases..

V. CONCLUSIONS

The rigid-flexible hybrid model of the bogie is established, and the bogie suspension system is equivalently simplified. According to the rigid-flexible hybrid model of the bogie, the mathematical model and experimental model of the bogie suspension system are established. The mathematical expression of the dynamic stiffness of the suspension is calculated from the mathematical model of the comprehensive dynamic stiffness test of the bogie suspension. Based on the test model of the bogie suspension system, the dynamic stiffness test of the bogie suspension system was carried out, and the vehicle suspension system test big data was obtained, thus the dynamic stiffness characteristic curve of the bogie suspension system was obtained with the bench test big data analysis.

(1) From the test results, the comprehensive dynamic stiffness of the bogie is found to vary nonlinearly with the frequency change in the range of 0.5∼5 Hz. The lateral dynamic stiffness of the suspension and the vertical dynamic stiffness of the suspension show a trend of decreasing first and then increasing with frequency, the trend of the decrease is due to the trend of the dynamic stiffness of the suspension. The longitudinal comprehensive dynamic stiffness of the suspension increases with an increase in frequency, and the stiffness tends to stabilize with increasing frequency at approximately 4 Hz.

(2) In the frequency range of 0.5∼5 Hz, the lateral dynamic stiffness of the primary suspension decreases with an increase in frequency. The longitudinal dynamic stiffness of the primary suspension initially increases with an increase in frequency, reaches a maximum value at approximately 4.5 Hz, then decreases. The vertical dynamic stiffness of the primary suspension initially decreases, then increases as the frequency increases, reaching a minimum value at approximately 3 Hz.

Based on the analysis, the occurrence of stiffness reduction is affected by the friction of a series of coil springs.

(3) In the frequency range of 0.5∼5 Hz, the transverse dynamic stiffness of the secondary suspension initially decreases and then increases as the frequency increases, reaching a minimum value at approximately 1 Hz. The longitudinal dynamic stiffness of the secondary suspension increases as the frequency increases. The vertical dynamic stiffness of the secondary suspension initially decreases, then increases as the frequency increases, reaching a minimum value at approximately 1.5 Hz.

ACKNOWLEDGMENT

Z. Niu would like to express appreciation to Dr. Huiying Lin and Dr. Yirui Zhang for valuable discussions that improved the quality and presentation of the paper.

REFERENCES

[1] H.-L. Shi, P.-B. Wu, and J. Zeng, "Flexibility characteristics of suspension system for railway vehicle," *J. Traffic Transp. Eng.*, vol. 14, no. 4, pp. 45–52, 2014.
[2] J. Zeng, "Numerical analysis of nonlinear stability for railway passenger cars," *Chin. J. Mech. Eng.*, vol. 14, no. 2, pp. 97–101, 2001.
[3] F. Li, M. H. Fu, and Y. H. Huang, "Research on car air spring dynamics parameter traits," *China Railway Sci.*, vol. 24, no. 5, pp. 91–95, 2003.
[4] H. Y. Liu, "Study on key dynamics problems of high-speed train," *China Railway Sci.*, vol. 25, no. 1, pp. 136–138, 2004.
[5] M. Piao, J. Ren, N. Li, and W. Zhao, "Comparative study on vertical vibration comfort of high-speed railway vehicle based on the suspension characteristics of air spring," *China Railway Sci.*, vol. 33, no. 1, pp. 71–77, 2012.
[6] W. J. Zhou, "Research on design of signgle-axle driving bogie," M.S. thesis, School Mech. Eng., Southwest Jiaotong Univ., Chengdu, China, 2008.
[7] W.-H. Ma, R.-R. Song, and S.-H. Luo, "Influence of journal box suspension parameters on dynamic performance of high-speed motor car," *Diesel Locomotives*, vol. 427, no. 9, pp. 15–19, 2009.
[8] H. Abdellatif and B. Heimann, "Computational efficient inverse dynamics of 6-DOF fully parallel manipulators by using the Lagrangian formalism," *Mechanism Mach. Theory*, vol. 44, no. 1, pp. 192–207, 2009.
[9] C. Mao-Ru, Z. Weihua, and Z. Jing, "Study of suspension parameter of high speed passenger car Bogies," *J. Dalian Jiaotong Univ.*, vol. 28, no. 3, pp. 13–19, 2007.
[10] K. H. A. Abood and R. A. Khan, "Railway carriage model to study the influence of vertical secondary stiffness on ride comfort of railway carbody running on curved tracks," *Modern Appl. Sci.*, vol. 5, no. 2, pp. 12–24, 2011.
[11] S. K. Sharma and A. Kumar, "Ride performance of a high speed rail vehicle using controlled semi active suspension system," *Smart Mater. Struct.*, vol. 26, no. 5, p. 055026, 2017.
[12] R.-H. Zhang, Z.-C. He, H.-W. Wang, F. You, and K.-N. Li, "Study on self-tuning tyre friction control for developing main-servo loop integrated chassis control system," *IEEE Access*, vol. 5, pp. 6649–6660, 2017.
[13] X. Sun, H. Zhang, W. Meng, R. Zhang, K. Li, and T. Peng, "Primary resonance analysis and vibration suppression for the harmonically excited nonlinear suspension system using a pair of symmetric viscoelastic buffers," *Nonlinear Dyn.*, vol. 94, no. 2, pp. 1243–1265, Oct. 2018, doi: 10.1007/s11071-018-4421-9.
[14] J. Zeng, J. Zhang, and Z. Shen, "Hopf Bifurcation and Nonlinear Oscillations in Railway Vehicle System," *Vehicle Syst. Dyn.*, vol. 33, no. 6, pp. 552–564, 1999.
[15] *Testing and Approval of Railway Vehicles from the Point of View of Their Dynamic Behavior-Safety-Track Fatigue-Ride Quality*, document UIC518, 2005.
[16] W.-H. Zhang, L.-Q. Chen, and L.-X. Huang, "Research on measurement method for vehicle parameters," (in chinese), *Rolling Stock*, vol. 38, no. 12, pp. 1–4, 2000.
[17] *Railway Applications-Ride Comfort for Passengers-Measurement and Evaluation*, document BS ENV 12299, 1999.
[18] M. Aizpun, A. Alonso, and J. Vinolas, "A new parameter identification methodology for the bogie rotational resistance test of a rail vehicle," *Proc. Inst. Mech. Eng. F, J. Rail Rapid Transit*, vol. 230, no. 3, pp. 879–890, 2016.
[19] W. Wang, Y. Zhao, and Y. Li, "Design and dynamic modeling of variable stiffness joint actuator based on archimedes spiral," *IEEE Access*, vol. 6, pp. 43798–43807, 2018.
[20] X. J. Kong *et al.*, "Mobility dataset generation for vehicular social networks based on floating car data," *IEEE Trans. Veh. Technol.*, vol. 67, no. 5, pp. 3874–3886, May 2018.
[21] S. M. M. Bideleh and V. Berbyuk, "Global sensitivity analysis of bogie dynamics with respect to suspension components," *Multibody Syst. Dyn.*, vol. 37, no. 2, pp. 145–174, 2016.
[22] F. Xia, A. Rahim, X. Kong, M. Wang, Y. Cai, and J. Wang, "Modeling and analysis of large-scale urban mobility for green transportation," *IEEE Trans. Ind. Informat.*, vol. 14, no. 4, pp. 1469–1481, Apr. 2018.
[23] Z. Q. Li, H. L. Li, and H. Y. Miu, "Development of a new rubber spring," *Railway Vehicles*, vol. 49, no. 4, pp. 12–14, 2011.
[24] Y. Feng, Z. Zhang, G. Tian, Z. Lv, S. Tian, and H. Jia, "Data-driven accurate design of variable blank holder force in sheet forming under interval uncertainty using sequential approximate multi-objective optimization," *Future Gener. Comput. Syst.*, vol. 86, pp. 1242–1250, Sep. 2018.
[25] G. Tian *et al.*, "Operation patterns analysis of automotive components remanufacturing industry development in China," *J. Clean Prod.*, vol. 164, pp. 1363–1375, Oct. 2017.
[26] G. Tian, M. Zhou, and P. Li, "Disassembly sequence planning considering fuzzy component quality and varying operational cost," *IEEE Trans. Autom. Sci. Eng.*, vol. 15, no. 2, pp. 748–760, Apr. 2018.
[27] Z. Qin *et al.*, "Influence of hydraulic shock absorber characteristic parameters on the critical speed of high-speed trains," *J. Mech. Eng.*, vol. 53, no. 6, pp. 138–144, 2017.
[28] A. Rahim *et al.*, "Vehicular social networks: A survey," *Pervasive Mobile Comput.*, vol. 43, pp. 96–113, Jan. 2018.
[29] X. J. Kong, X. Song, F. Xia, H. Guo, J. Wang, and A. Tolba, "LoTAD: Long-term traffic anomaly detection based on crowdsourced bus trajectory data," *World Wide Web*, vol. 21, no. 3, pp. 825–847, 2017.
[30] Q. Ji, "Research on performance parameter test rig of freight car," M.S. thesis, School Mech. Eng., Southwest Jiaotong Univ., Chengdu, China, 2005.
[31] X. Kong, M. Li, T. Tang, K. Tian, L. Moreira-Matias, and F. Xia, "Shared subway shuttle bus route planning based on transport data analytics," *IEEE Trans. Automat. Sci. Eng.*, vol. 15, no. 4, pp. 1507–1520, Oct. 2018, doi: 10.1109/TASE.2018.2865494.
[32] H. Xiong, X. Zhu, and R. Zhang, "Energy recovery strategy numerical simulation for dual axle drive pure electric vehicle based on motor loss model and big data calculation," *Complexity*, vol. 2018, Aug. 2018, Art. no. 4071743, doi: 10.1155/2018/4071743.
[33] Z. Y. He, "Simulation analysis of influences of anti-roll torsion bar on vehicle dynamics," *Appl. Mech. Mater.*, vols. 409–410, no. 4, pp. 1486–1491, 2013.
[34] Z. Qi, F. Li, Y. Huang, and D. Yu, "Study on the pneumatic simulation model of railway vehicle air spring system based on AMESim," *China Railway Sci.*, vol. 34, no. 3, pp. 79–86, 2013.
[35] J. Chen, "Study on modelling and dynamic characteristic of air spring with throttling damping orifice and auxiliary chamber," *J. Mech. Eng.*, vol. 53, no. 8, pp. 166–174, 2017.
[36] Y.-R. Zhang, J. Su, L. Zhang, F.-X. Tan, and G. Xu, "Primary suspension stiffness testing of railway vehicle bogie," *J. Jilin Univ. (Eng. Technol. Ed.)*, vol. 46, no. 4, pp. 1083–1089, 2016.
[37] H. Shi, Y. Song, P.-B. Wu, J. Zeng, and H.-Y. Zhu, "Calculation and testing of suspension stiffness of a bogie of high speed EMU," *J. Jilin Univ. (Eng. Technol. Ed.)*, vol. 45, no. 3, pp. 776–782, 2015.
[38] H.-L. Shi, P.-B. Wu, R. Luo, and J.-Y. Guo, "Calculation and laboratory testing of the rotation resistance of a bogie," *Proc. Inst. Mech. Eng. F, J. Rail Rapid Transit*, vol. 229, no. 2, pp. 210–219, 2015.
[39] G. W. Zhou, J. X. Wang, and Y. Zhou, "Experimental study on the dynamic stiffness and damping of water lubricated rubber bearings," *J. Sichuan Univ.*, vol. 46, no. 3, pp. 193–198, 2014.
[40] B. F. Zong, C. M. Chu, and G. Miao, "Vibration characteristic analysis of transmission case based on vibration transfer function," *Agricult. Equip. Vehicle Eng.*, vol. 55, no. 4, pp. 43–46, Apr. 2017.
[41] F. Xia, J. Wang, X. Kong, Z. Wang, J. Li, and C. Liu, "Exploring human mobility patterns in urban scenarios: A trajectory data perspective," *IEEE Commun. Mag.*, vol. 56, no. 3, pp. 142–149, Mar. 2018.

[42] A. Matsubara, R. Sawamura, K. Asano, and T. Muraki, "Non-contact measurement of dynamic stiffness of rotating spindle," *Procedia CIRP*, vol. 14, pp. 484–487, Mar. 2014.
[43] L. E. Ooi and Z. M. Ripin, "Dynamic stiffness and loss factor measurement of engine rubber mount by impact test," *Mater. Des.*, vol. 32, no. 4, pp. 1880–1887, 2011.
[44] Q.-G. Hu, H. Zhou, T.-H. Luo, T. Peng, and Z.-Y. Tian, "Analysis of static and dynamic characteristics of rubber mounts of large dump truck," *Machinery Des. Manuf.*, vol. 12, pp. 213–215, Dec. 2015.
[45] S. S. Rao, *Mechanical Vibrations*. Reading, MA, USA: Addison-Wesley, 1990.
[46] T. Yagi, A. Stensson, and C. Hardell, "Simulation and visualisation of the dynamic behaviour of an overhead power system with contact breaking," *Vehicle Syst. Dyn.*, vol. 25, no. 1, pp. 31–49, 1996.
[47] S. D. Iwnicki and A. H. Wickens, "Validation of a MATLAB railway vehicle simulation using a scale roller rig," *Vehicle Syst. Dyn.*, vol. 30, nos. 3–4, pp. 257–270, 1998.

ZHIHUI NIU received the B.S. degree in transportation from the Shandong University of Technology, Zibo, China, in 2012. He is currently pursuing the Ph.D. degree with the Transportation College, Jilin University, Changchun, China. His research interests mainly engaged in intelligent detection and diagnosis.

JIAN SU received the master's degree from Jilin University, Changchun, China, in 1994. He has authored or co-authored over 86 papers. He held 120 national invention patents. He has hosted two projects supported by the National Science and Technology Support Program and the National 863 Plan, two projects supported by the National Natural Science Foundation, and 14 projects supported by the National Science Foundation of Jilin Province. He has completed over 40 research projects in total. He received the National Invention Patent Excellence Award, the Jilin Province Patent Excellence Award, and the Pittsburgh International Invention Exhibition Invention Award. He was a recipient of the Jilin Province Science Award.

YINRUI ZHANG received the B.S. degree in transportation from the Shandong University of Technology, Zibo, China, and the M.S. and Ph.D. degrees in automobile application engineering from Jilin University, Changchun, China. His research interests mainly engaged in intelligent detection and diagnosis.

HUIYING LIN received the Ph.D. degree from Jilin University, Changchun, China, in 2008, and the Ph.D. degree with the Transportation College, Jilin University. Her research interests mainly engaged in intelligent detection and diagnosis.